Nanoscale

Accepted Manuscript

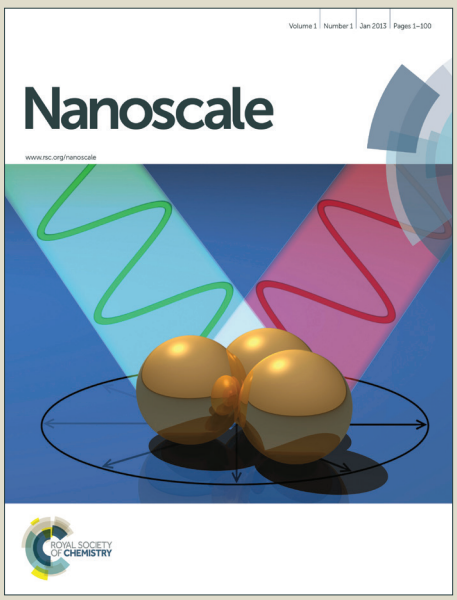

ROYAL SOCIETY OF CHEMISTRY

www.rsc.org/nanoscale

Nano Scale Nanoscale Dynamic Article Links►

Cite this: DOI: 10.1039/c0xx00000x

www.rsc.org/xxxxxx

PAPER

Combined toxicity study of zinc oxide nanoparticles and Vitamin C in food additives

Yanli Wang[a], Lulu Yuan[a], Chenjie Yao[a], Lin Ding[a], Chenchen Li[a], Jie Fang[a], Keke Sui[a],Yuanfang Liu[b]*, Minghong Wu[a]*

Received (in XXX, XXX) Xth XXXXXXXXX 20XX, Accepted Xth XXXXXXXXX 20XX
DOI: 10.1039/b000000x

At present, safety evaluation standards for nanofood additives are made based on the toxic effect of single additive. Since the size, surface properties and chemical nature influence the toxicity of nanomaterials, the toxicity may have dramatically changed when nanomaterials are used as the food additives in a complex system. Herein, we investigated the combined toxicity of zinc oxide nanoparticles (ZnO NPs) and Vitamin C (Vc, ascorbic acid). The results showed that Vc increased the cytotoxicity significantly compared with that of the single ZnO NPs. When the cells were exposed to ZnO NPs at a concentration less than 15 mg/L, or to Vc at a concentration less than 300 mg/L, there was no significant cytotoxicity, both in the case of GES-1 and NSCs. However, when the 15 mg/L of ZnO NPs and 300 mg/L of Vc were introduced to cells together, the cell viability decreased sharply indicating significant cytotoxicity. Moreover, the significant increase of toxicity was also shown in the *in vivo* experiments. The dose of ZnO NPs and Vc used in the *in vivo* study was calculated according to the state of food and nutrition enhancer standard. Mice after repeated oral exposure to ZnO NPs plus Vc, the injury of liver and kidneys has been indicated by the change of these indices. These findings demonstrate that the synergistic toxicity presented in a complex system is essential for the toxicological evaluation and safety assessment of nanofood.

Introduction

Nanotechnology has the potential to make food healthier, safer and better tasted, and improve the antibacterial packaging of food that creates a rapidly growing category of food called nanofood. [1] However, the potential risk of the nanofood has aroused the serious concerns in public and academia. Many organizations have called for cautious application and some consumers tend to reject the related products. [2] In 2011, the European Parliament called for further checks of the adequate safety assessment of nanofood. Also, that the food containing nano-ingredients should be labelled was wanted. Unfortunately, in most cases, the market does not follow, intentionally or unintentionally, the new rule for nanofood, usually there are no specific labels indicating the nanomaterials added in food. Furthermore, at present the safety evaluation standards for nanofood additives are set up only based on the toxic effects of a single nano-additive in a simple system of food. The combined effects of the nonsingle additives in a complex system of nanofood remain unknown. [3]

Since the size, surface properties and chemical nature influence the toxicity of nanomaterials, [4-8] these toxicity may have dramatically changed when nanomaterials are used as the food additives in a complex system. Therefore, we should pay particular attention to the combined effects of nanomaterials additives and other additive. There are few reports about the combined effects of nanoparticles. Martirosyan *et al*. concluded that in the presence of quercetin and kaempferol, the toxicity induced by Ag nanoparticles was partially down-regulated in Caco-2 cells. [9] Guo *et al*. found that co-exposure to carbon black and Fe_2O_3 nanoparticles caused a synergistic oxidative effect in cultured lung epithelial cells while exposure to either particle type alone did not. [10] Unfortunately, so far there is no any related research on the combined toxicity of nonsingle nanoparticles additives in food. Currently, metal oxide nanoparticles are

receiving increasing attention for a large variety of applications. Major metal oxides nanoparticles of zinc, titanium, silica and copper are showing promise in food safety and technology. [11, 12] ZnO NPs are currently listed as the generally recognized as safe (GRAS) material by the Food and Drug Administration and are allowed to be used as food additive. It is very well known that zinc is a most important essential trace element for human beings, there are hundreds of functional enzymes containing Zn in the body. [13, 14, 15] Thus, Zn is widely used as a nutritious supplement of trace element, particularly needed for kids. [13, 16] Meanwhile, due to the pronounced antimicrobial property of Zn, ZnO NPs are also commonly used as an effective ingredient for longer preservation and shelf life of food. [17, 18] However, lots of literatures showed that ZnO NPs up to a proper concentration were toxic to cells, such as *Tetrahymena thermophila,* [19] *Escherichia coli,* [17] NIH3T3 and human lung A549 cell line. [20] Cells exposed to ZnO NPs led to dose- and time-dependent cytotoxicity which was reflected in oxidative stress, lipid peroxidation, cell membrane damage, and oxidative DNA damage. And ZnO NPs exhibited a much steeper dose-response pattern unseen in other metal oxides. [21-23] Vitamin C (ascorbic acid, (R)-3,4-dihydroxy-5-((S)-1,2dihydroxyethyl)furan-2(5H)-one) is a vital nutritious compound with many beneficial functions for humans. Most importantly, it acts as a potent water-soluble antioxidant in biological fluids [24, 25] for the synthesis and function of immune system factors by scavenging physiologically relevant reactive oxygen species and reactive nitrogen species. [26, 27] Hence, Vc are often added into many food, and also taken up from vegetables and fruits in order to enhance the human immunity and health. [18, 28]

Herein, we employed ZnO NPs with different size and surface properties and took gastric epithelial cell line (GES-1) and neural stem cells (NSCs) as cellular models to study the combined cytotoxicity of ZnO NPs plus Vc. In addition, we further took mice to study the *in vivo* combined toxic effects. Our findings may reach a verdict that the remarkable synergistic toxicity happens in the complex system of ZnO NPs plus Vc.

Results and Discussion

1. Characterization of ZnO NPs

The TEM images (Fig.1) show the size and morphology of ZnO NPs. Other physicochemical properties of ZnO NPs are summarized in Table S1 (ESI, Table S1†). The purities of these NPs are higher than 95 % according to X-ray fluorescence (XRF) analyses. Based on the X-Ray diffraction (XRD) patterns (ESI, Fig. S1†), ZnO NPs can be indexed to hexagonal wurtzite structure of ZnO, which are in good agreement with the standard JCPDS file of ZnO (JCPDS Card No. 36-1451). From TEM images we can see that the sizes of ZnO-NPs are different. However, there is no big difference of the sizes of ZnO-NPs in water or in medium (ESI, Table S1†).

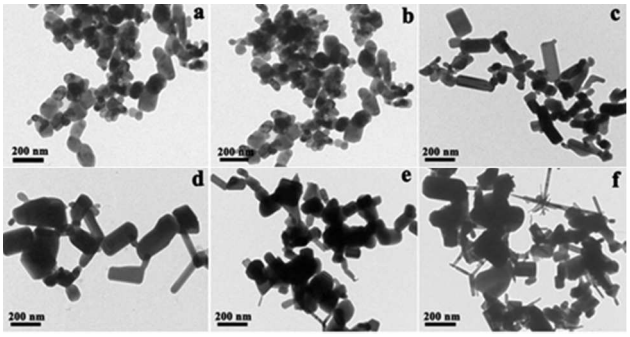

Fig. 1 TEM images of ZnO NPs. (a) ZnO-1; (b) ZnO-2; (c) ZnO-3; (d) ZnO-4; (e) ZnO-5; (f) ZnO-6.

2. Cytotoxicity study

CCK-8 assay was employed to compare the viability of GES-1 and NSCs after co-incubation with different concentrations of ZnO NPs, Vc and ZnO NPs plus Vc. Studies have shown that when the concentration of ZnO NPs is less than 15 mg/L or the concentration of Vc is less than 300 mg/L, there is no significant toxicity to GES-1 and NSCs, cell viability is high than 90 % for both. However, when 15 mg/L ZnO NPs and 300 mg/L Vc are introduced to cells together, Vc increases the cytotoxicity (GES-1 and NSCs) of ZnO-NPs significantly, the cell viability decreases to about 55%, 30%, 23%, 20%, 24%, 22% in GES-1 and 38%, 21%, 22%, 23%, 20%, 18% in NSCs, respectively (Fig. 2a,b).

The same cytotoxicity increase trend happens when co-incubation with different concentrations of ZnO NPs (ESI, Fig. S2†). Even at the lower concentration of 10 mg/L, the combined toxicity also shows the strong decrease effects on the cell viability. To quantitatively study the combined effects of ZnO NPs plus Vc, flow cytometry was employed to detect apoptotic and necrotic cells. Because all kinds of ZnO NPs used in this study show the similar effect trend, we chose one sample to do the following experiment to further confirm the combined effect of ZnO NPs plus Vc. Based on apoptosis experiment results we found that Vc (300 mg/L) and ZnO-5 (15 mg/L) do not cause early apoptosis, but the group of ZnO-5 (15 mg/L) plus Vc (300

mg/L) cause early apoptosis significantly compared with control group after co-incubation with cells for 24 h (Fig. 3(a-h)). For GES-1 cells the apoptosis rate is as high as 52.17%, mortality rate is 5.46% (Fig. 3 (a-d)); for NSCs, the apoptosis rate is as high as 51.38%, mortality rate is 9.44% (Fig. 3(e-h)).

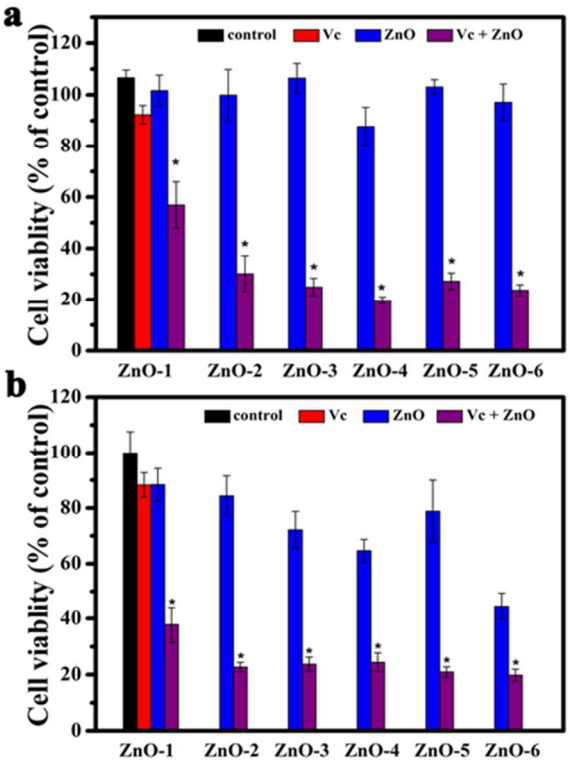

Fig. 2 Cytotoxicity evaluation of ZnO NPs (15 mg/L), Vc (300 mg/L) and ZnO NPs plus Vc treatment for 24 h. (a) Cell viability analysis of GES-1 after co-incubation with ZnO NPs, Vc and ZnO NPs plus Vc treatment for 24 h; (b) Cell viability analysis of NSCs after co-incubation with ZnO NPs, Vc and ZnO NPs plus Vc treatment for 24 h. *p < 0.05 compared with cells exposed to ZnO NPs.

Calcium plays an important role in the regulation of cell apoptosis. Subtle changes of the concentration of calcium in the subcellular distribution can effectively regulate the cell apoptosis. [29] Fluo-3 probes are used to detect the effect on the concentration of Ca^{2+} in cells. GES-1 (Fig. 3 (i-l)) and NSCs (Fig. 3 (m-p)) are exposed to ZnO-5 (15 mg/L), Vc (300 mg/L) and ZnO-5 (15 mg/L) plus Vc (300 mg/L). The concentration of Ca^{2+} in cells keep unchanged after co-incubation with ZnO-5 (15 mg/L) and Vc (300 mg/L) for 2 h. But after cells co-incubation with ZnO-5 (15 mg/L) plus Vc (300 mg/L) for the same time, the concentration of Ca^{2+} increased significantly. Shao *et al.* found that in primary cultured rat cerebral cortical cells that chronic treatment with valproate, as well as lithium, reduced the Ca^{2+} by buffering the overloaded intracellular calcium, hence stabilizing mitochondria function and inhibiting production of reactive oxygen species. [30]

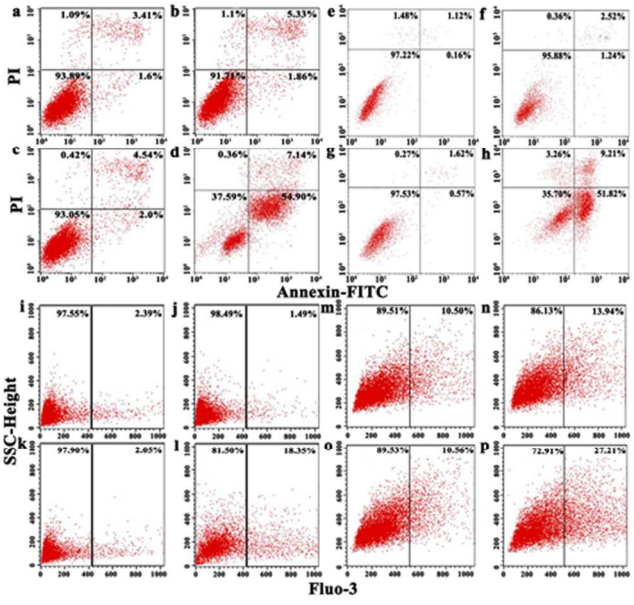

Fig. 3 Cytotoxicity evaluation of ZnO NPs (15 mg/L), Vc (300 mg/L) and ZnO NPs plus Vc treatment for 24 h. (a-h) The combine d effect of ZnO NPs and ZnO NPs plus Vc on apoptosis/necrosis after 24 h incubation: (a-d) GES-1, (e-h) NSCs, (a, e) Control, (b, f) 15 mg/L ZnO NPs, (c, g) 300 mg/L Vc, (d, h) 300 mg/L Vc plus 15 mg/L ZnO NPs; (i-p) Quantification analysis of calcium ion concentration in GES-1(i-l) and NSCs (m-p) after incubated with ZnO NPs, Vc and Vc plus ZnO NPs for 2 h: (i, m) control, (j, n) 15 mg/L ZnO NPs; (k, o) 300 mg/L Vc; (l, p) 15 mg/L ZnO-5 plus 300 mg/L Vc.

Since cytotoxicity is closely related to the oxidative stress in cells, we have measured the level of ROS in GES-1. [31] The results in Fig. 4a show that GES-1 exposed to 15 mg/L ZnO NPs and 300 mg/L Vc for 24 h, resulting in a significant increase in the generation of ROS and there was no generation change of ROS in GES-1 treated with 300 mg/L Vc or 15 mg/L ZnO NPs. Mitochondria are central to both normal cell function and the regulation of cell death, and also the primary intracellular source of ROS. [32] Apoptosis can be activated by different signaling pathways, and the opening of the permeability transition pore (PTP) and a subsequent drop in mitochondrial membrane potential (MMP) are recognized as the main mechanisms. [33] Herein, we investigated the effects of ZnO NPs plus Vc on GES-1' MMP. From Fig. 4b, the MMP of GES-1 treated with 15 mg/L ZnO NPs plus 300 mg/L Vc for 24 h dropped to about 40% of control.

Caspases, the cytoplasmic aspartate-specific cysteine proteases, represent the apoptotic-related proteins, to which most of the death signals converge to induce apoptosis. Caspases

activated by the released cytochrome C can enter mitochondria to cleave key substrates in the mitochondrial electron transport chain, leading to the increased production of ROS. [34] We had measured the activity of casapase-3 in GES-1 and NSCs with the results presented in Fig. 4 (c, d). ZnO NPs plus Vc induce the high-regulation of the activity of caspase-3 compared with control in both GES-1 and NSCS, but the ZnO NPs or Vc treated cells remained almost equal to control. These findings, taken together, indicate that the synergistic toxic effects of ZnO NPs plus Vc involve ROS and mitochondria linked signal pathway.

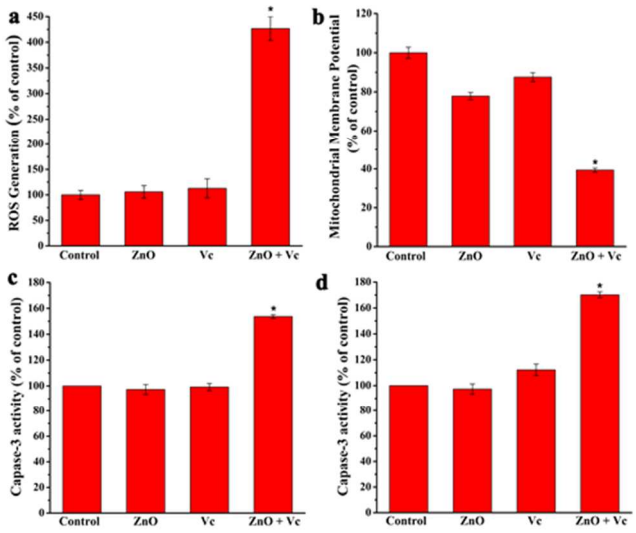

Fig. 4 Cellular apoptosis evaluation after ZnO NPs (15 mg/L), Vc (300 mg/L) and 15 mg/L ZnO NPs plus 300 mg/L Vc treatment for 24 h. (a) ROS generation in GES-1; (b) MMP in GES-1; (c) caspase-3 activity evaluation in GES-1; (d) caspase-3 activity evaluation in NSCs. *p < 0.05 compared with cells exposed to ZnO NPs.

GES-1 (Fig. 5) and NSCs (ESI, Fig. S3†) cells damages induced by ZnO NPs and ZnO NPs plus Vc were shown by cellular and nuclear morphological changes. Results showed that the cells grew well in the control group, ZnO-5 (15 mg/mL) group and Vc (300 mg/L) group. Cells exhibited normal cell morphology, integrity and nuclear size. However, cells treated with ZnO NPs (15 mg/L) plus Vc (300 mg/L) were rounded up and exhibited typical apoptosis features displayed as cell body shrinkage, nuclear condensation and loss in cell membrane integrity. These results further demonstrated that Vc could increase the cytotoxicity of ZnO NPs. Our investigation showed that exposure to ZnO NPs and Vc made the viability of GES-1 and NSCs declined sharply, and the membrane integrity and the apoptosis of GES-1 and NSCs correspondingly increased sharply.

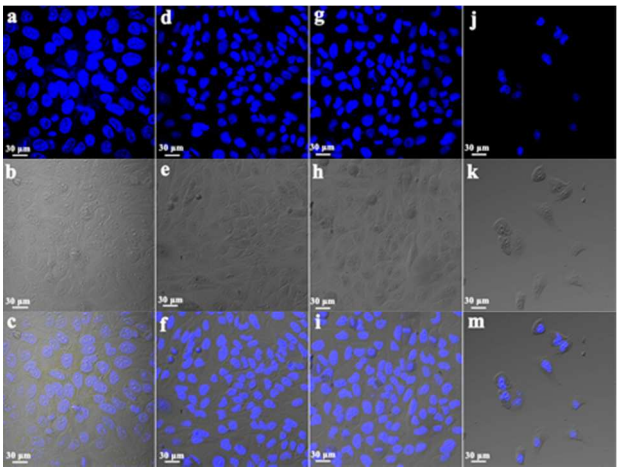

Fig. 5 Observation of the morphological changes of GES-1 after treatment with ZnO NPs, Vc and ZnO NPs plus Vc. (a, b, c) control; (d, e, f) 15 mg/L ZnO NPs; (g, h, i) 300 mg/L Vc; (j, k, m) 15 mg/L ZnO NPs plus 300 mg/L Vc. (a, d, g, j) stained by DAPI; (b, e, h, k) in the bright-field; (c) merge of (a) and (b); (f) merge of (d) and (e); (i) merge of (g) and (h); (m) merge of (j) and (k).

2. Mechanism study on the combined cytotoxicity effects

The toxic effects of ZnO NPs to cells was caused by their dissociated and solubilised fraction Zn^{2+} ions, which disrupts cellular zinc homeostasis, leading to lysosomal and mitochondria damage and ultimately cell death. [19, 35-37] Toxicity of ZnO NPs to bacteria vibrio fischeri and crustacean thamnocephalus platyurus was also caused by dissolved Zn^{2+}. [36] Therefore, we measured the quantity of Zn^{2+} in cells. TSQ is a commonly used Zn^{2+} sensor. Zn^{2+} binding is accompanied by the appearance of an intense fluorescence emission spectrum. TSQ and its related fluorophores are bidentate ligands, utilizing quinoline and sulfonamide nitrogens to coordinate Zn^{2+}. [38] There is no fluorescence from zinc ions except for the background fluorescent color in the control group. Under the same voltage, the cells treated with ZnO NPs or Vc are in normal cell morphology and integrity. The obvious blue colour of Zn ion was present in GES-1 co-incubated with ZnO NPs, but no toxicity was induced by ZnO NPs. However, after co-incubation with ZnO NPs plus Vc, cells are rounded (ESI, Fig. S4†), and the average fluorescence intensity is much higher than the cells co-incubated with ZnO NPs (Fig. 6). Conclusively, in Fig. 6, the average intensity of cells treated with ZnO NPs for 2 h is 466; for 24 h is 316, ZnO NPs plus Vc for 2 h is 705 and 1184 for 24 h. Additionally, we used flow cytometry to study the amount of zinc ion in GES-1 in Fig 6 (b-e), there are two gates in the figure, the left gate shows the viable cells and the right gate stands for the nonviable cells stained by TSQ. Obviously, the cells treated by ZnO NPs plus Vc produce more

zinc ion and appear apoptosis (Fig. 6e). By the data mentioned above, the increased cytotoxicity of ZnO NPs plus Vc is further confirmed. And the increased concentration of Zn^{2+} in cells is a dominating factor making the cytotoxicity increased sharply.

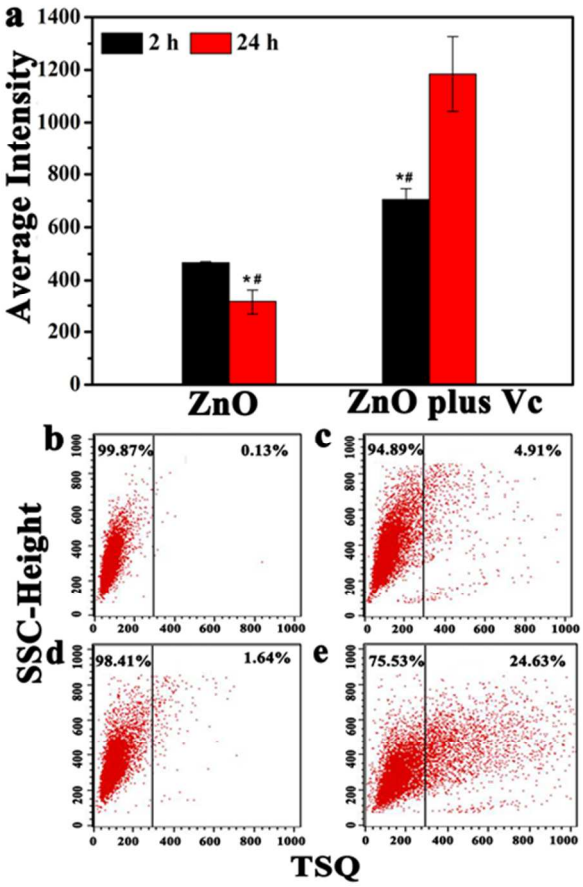

Fig. 6 Analysis of average fluorescent intensity of zinc ion in GES-1 after incubated with ZnO NPs and ZnO NPs plus Vc for 2 h and 24 h respectively. (a) The average fluorescent intensity of zinc ion in GES-1 after treated with ZnO NPs and ZnO NPs plus Vc; (b-e) quantitative analysis of zinc ion in GES-1 by flow cytometry after incubation for 2 h. (b) control; (c) 15 mg/L of ZnO NPs; (d) 300 mg/L of Vc; (e) 15 mg/L of ZnO-5 plus 300 mg/L of Vc. *p < 0.05 compared with cells exposed to ZnO NPs for 2 h, #p < 0.05 compared with cells exposed to ZnO NPs plus Vc for 24 h.

To view how Vc increases the concentration of Zn^{2+} in cells, we studied the uptake and sub-cellular location of ZnO NPs and Zn^{2+}. From Fig. 7, we can see that ZnO NPs first concentrate on cell membrane than traverse through the membrane and translocate into cell cytoplasm. After 2h-incubation, most of the ZnO NPs locate in lysosome both for ZnO NPs and ZnO NPs plus Vc treated group. With incubation time prolonging to 24 h, part of ZnO NPs dissolve into Zn^{2+} in cells, and there are much lower concentration of Zn^{2+} in ZnO NPs treated group than ZnO NPs plus Vc treated group. Mechanically, ZnO NPs can dissolve under aqueous condition to form hydrated Zn^{2+}, this dissolution increases under acidic conditions as well as the presence of biological components such as amino acids and peptides. [39, 40] The acidity of ascorbic acid enhances the release of Zn ions from ZnO NPs to aqueous medium, hence inducing more serious cytotoxicity. This is a predominating mechanism for the increase of Zn ions affected by ascorbic acid. Furthermore, in literature, endocytosis and intracellular trafficking of different NPs have been reported. The mechanism and influencing factors of endocytosis have been discussed extensively. [5] The endocytosis of NPs is affected by a variety of factors, such as the composition, size, shape and surface properties of NPs [41-48]. Form our results we infer that Vc increases the endocytosis rate and ratio of ZnO NPs by changing the size and zeta potential and also promote dissolution rate of ZnO NPs in cells which may be the main factor to contribute to the increase of Zn^{2+} in cells (ESI, Fig. S5†).

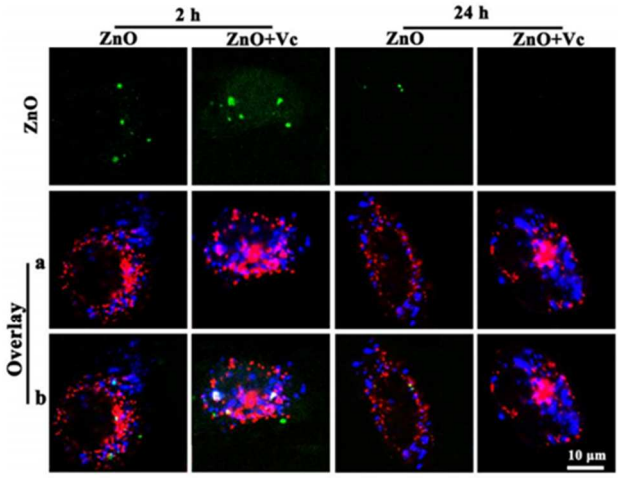

Fig. 7 Measurement of Zn ion and ZnO NPs in GES-1 after incubated with 15 mg/L ZnO-NPs, 15 mg/L ZnO NPs plus 300 mg/L Vc for 2 h and 24 h respectively. (a) overlay of TSQ (blue) and lysosome (red); (b) overlay of TSQ, FITC-ZnO NPs (green) and lysosome.

3. Synergistic toxicity *in vivo*

The issue is exacerbated when mechanistic data obtained from *in vitro* experiments are directly translated to human hazard and used for risk assessment. This can lead to information that is taken out of experimental context and reported as a definitive effect in humans. Care must be exercised when extrapolating the *in vitro* findings to *in vivo* effects. [49] To avoid misleading information provided by the *in vitro* findings that is not causally linked to *in vivo* events in animals or in humans. We further investigated the combined toxicity of ZnO NPs and Vc in mice via oral injection twice a day for 30 days and 90 days. The

injection doses of ZnO NPs and Vc calculated according to the state of food and nutrition enhancer standard. The doses for mice are adjusted according the equivalent dose ratio of mouse to human beings for 9:1. First, we investigated the biochemical index of serum and blood (ESI, Table S2†). The interesting and important result is that the combined toxicity of ZnO NPs plus Vc *in vivo* show age-dependent trend. In the first group mice in 5-6 weeks old, ALP shows significant difference compared with control group. At the same condition, there are no any changes of index of liver function for the young mice in 3-4 weeks old (Fig. 9a). And the weight gain treated with ZnO NPs plus Vc also shows the significant difference (Fig. 8a). However, ZnO NPs and ZnO NPs plus Vc have little influence on the body weight of adult mice (Fig. 8c, e). In Fig. 8b and 8d, the bio-distribution is different after treated with ZnO NPs and ZnO NPs plus Vc. ZnO NPs plus Vc treated group shows high accumulation of Zn in the main organs compared with ZnO NPs treated group for the adult mice. For younger mice group, the bio-distribution shows a contrary tendency. With the time prolonging, the accumulation of Zn in the main organs show slight change (Fig. 8f). Shimamura *et al*. investigated the aging effects on the concentrations of 26 major to trace elements and mutual elemental relationships. The concentration of many elements including Zn, showed significant increasing trends (*p < 0.05) with different ages. [50]

We prolong the exposure time to 90 days, the main index of liver and kidney such as total bilirubin levels (TBIL) and blood urea nitrogen (BUN) show significant change compared with control (Fig. 9 (b, c)). Further, by mRNA reverse transcription-polymerase chain reaction (RT-PCR) technique. The liver fatty acid binding protein (L-FABP), neutrophil gelatinase associated lipocalin (NGAL) and apolipoprotein (APO) are investigated. NGAL is a marker of renal tubular injury. L-FABP and APO play very important roles in liver and be related with the hepatitis. [51-53] In Fig. 9 (d-f), L-FABP, APO and NGAL, which directly relate with the function of liver and kidneys, show significant change after treated with ZnO NPs plus Vc.

Since the adverse effects of environmental nanoparticles, so called ultrafine particles in the past, have already been widely reported, thus consumers worry about the potential risks very much when using products containing nanoparticles. [54, 55] At present, various nanomaterials have directly come into contact of consumers, particularly through the nanofood. Responding to the serious concerns on the potential adverse effects to human health, surrounding applications of nanotechnology some form of legislation may be enacted in the near future.

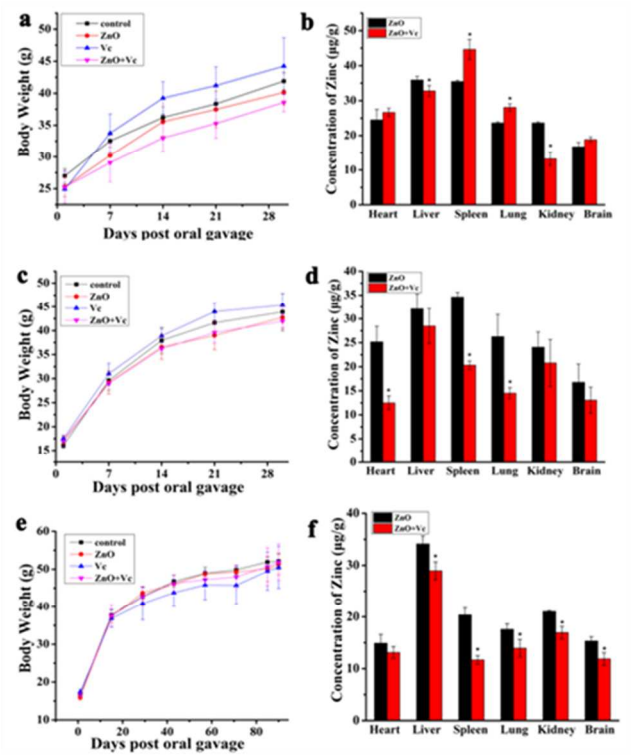

Fig. 8 The dynamic curves of body weight change and the content of Zinc in each tissue after treated with ZnO NPs, Vc and ZnO NPs plus Vc. (a, b) first group of adult mice (5-6 weeks old) treated with different samples for 30 days; (c, d) second group of young mice (3-4 weeks old) treated with different samples for 90 days; (e, f) third group (3-4 weeks old) treated with different samples for 90 days. #P<0.05 compared with control. *p< 0.05 compared with cells treated with ZnO-5 alone.

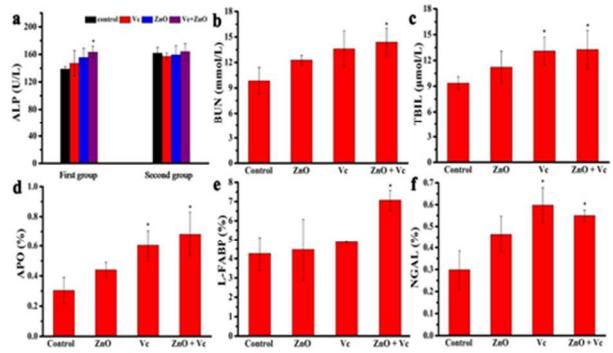

Fig. 9 (a, b, c) The serum biochemical parameters and expression of mRNA of liver and kidney: (a) ALP of the first group and second group mice; (b) BUN of the third group mice; (c) TBIL of the third group mice; (d, e, f) The relative mRNA expression in liver and kidney of the third group mice. *p< 0.05 compared with control.

Our results of both *in vitro* and *in vivo* experiments have definitely showed that Vc increases the toxicity of ZnO NPs.

However, we find that an analogous metal oxide NPs (TiO_2 NPs), which is more chemically inert, seems much less toxic, even in a complex system containing Vc. (ESI, Fig. S6†, S7†, S8†, Table S3†). Overall, for the safety assessments of nanofood, the nanotoxicological study of the composite systems requires more efforts in the future.

Experimental Section

Materials: Six kinds of ZnO NPs were used in this study, namely ZnO-1, ZnO-2 (Hydratight nanomaterials Co., Ltd. Nanjing, China), ZnO-3, ZnO-4 (Wan Jingxin materials Co., Ltd. Hangzhou, China), ZnO-5 (Wuxi Zehui Chemical industry Co., Ltd. Jiangsu, China) and ZnO-6 (Haishun Xinye Co., Ltd. Zibo, China).

Characterization of NPs: The crystalline phase of ZnO NPs were analyzed by XRD (Rigaku Co., Tokyo, Japan). The shape and size of ZnO NPs were investigated by TEM (JEM-200CX, JEOL, Japan). The purity of NPs was analyzed using XRF (S4-Explorer, Bruker, Germany). The hydrodynamic size of the NPs in water and culture medium and the zeta potential in water were measured on a Nanosizer (Zetasizer 3000 HS, Malvern, UK).

Cell culture: GES-1 cells were obtained from the Chinese Academy of Sciences. NSCs were kindly provided by Prof. Wen T.Q. (Shanghai University, China). Dulbecco's modified Eagle's medium (DMEM) and fetal bovine serum were purchased from Gino Biological Pharmaceutical Technology co., Ltd (Hangzhou, China). Cells were grown to confluence in 25 cm^2 flasks supplemented with high-glucose DMEM and 10% FBS, and incubated in a humidified incubator with 5% CO_2 and 95% air at 37 °C. Eighty percent of confluent cells were used in all the assays.

Toxicity assay in vitro

Cell proliferation: Cell viability assays were performed using a CCK-8 Kit (Dojindo Laboratories, Japan) following the manufacturer's instructions. The cell viability was expressed as the percentage of viable cells of the total cells. Briefly, cells were seeded in 96-well plates (3×10^3 cells per well), after a 24 h incubation period, cells were treated with different concentrations of ZnO NPs, Vc and ZnO NPs plus Vc; TiO_2 NPs, Vc and TiO_2 NPs plus Vc for an additional 24 h. The cell viability of each well was determined with the CCK-8 kit following the instruction manual and the 450 nm absorbance of each well was measured using a microplate reader (Thermo, USA).

Annexin V-FITC and PI assays: Annexin V-FITC and propidium iodide (PI) assays were employed to detect apoptotic and necrotic cells. Stained cells were analyzed by two-color flow cytometry. The assay procedure was performed according to the instruction manual of the annexin V-FITC kit I (BD Biosciences, USA). After co-incubation for 24 h of ZnO-5 (15 mg/L), Vc (300 mg/L) and ZnO-5 (15 mg/L) plus Vc (300 mg/L), the cells were harvested, washed twice with cold phosphate-buffered saline (PBS 0.15 M, PH=7.2) and resuspended to 1×10^6 cells/mL in a mixed buffer. Next, 100 μL cells was transferred to a 5 mL culture tube and 5 μL FITC-conjugated annexin V (Annexin V-FITC) and 5μL PI were added at room temperature. After incubation for 15 min at room temperature in the dark, stained cells were diluted using the mixed buffer and directly analyzed by flow cytometry (FACS, BD Biosciences, USA).

Quantification of Ca^{2+} in GES-1: To study the intracellular concentrationof Ca^{2+}, GES-1 treated with 15 mg/L ZnO-5, 300 mg/L Vc and 15 mg/L ZnO-5 plus 300 mg/L Vc for 2 h were loaded with 10 μM Fluo-3 AM (Beyotime) for 30 min at 37 °C and followed by washing with D-PBS for three times. Then the cells were incubated for another 20 min to ensure complete cleavage of Fluo-3 AM by the intracellular ester enzyme that released Fluo-3 before the illumination. After that, stained GES-1 were directly analyzed by flow cytometry (FACS, BD Biosciences, USA).

DNA fluorescent staining and confocal laser scanning microscopy studies: The fluorescent probe 4, 6-diamidino-2-phenylindole (DAPI) is a popular nuclear counter stain in multicolor fluorescent techniques. It stains nuclei specifically, with little or no cytoplasm labeling. [56] GES-1 and NSCs were pre-cultured in culture medium containing 15 mg/L of ZnO-5, 300 mg/L Vc and ZnO-5 (15 mg/L) plus Vc (300 mg/L) for 24 h. Subsequently, cells were rinsed by PBS and DAPI solutions. The cells were kept in a 2 mg/L DAPI solution for 15 min in the dark at room temperature. Finally, the cells were washed twice with PBS to remove excess DAPI and examined under a confocal microscope (FV1000, Olympus Corp., Tokyo, Japan) with an excitation wavelength of 405 nm.

Fluorescence assessment of zinc ions and cell morphology

Analysis of fluorescence of Zn^{2+} in GES-1: A commonly used Zn^{2+} fluorophore is 6-methoxy-8-p-toluenesulfonamido-quinoline (TSQ) (Shanghai Meilian Biotechnology Co., Ltd, China). We used a method developed by Meeusen for this assay. [38] Briefly, GES-1 were pre-cultured in culture medium containing 15 mg/L of ZnO-5 and ZnO-5 (15 mg/L) plus Vc (300 mg/L) for 2 h or 24 h. The cells were then rinsed three times with PBS and stained for 30 min in an incubator using a solution of 30 μM TSQ in PBS. After the stained cells were rinsed three times with PBS, the cells were examined under a confocal microscope (FV1000, Olympus Corp., Tokyo, Japan) with an excitation wavelength of 405 nm. Then, we used confocal to analyze the average fluorescence intensity of Zn^{2+} in GES-1.

Quantification of Zn^{2+} with flow cytometry: Briefly, GES-1 were pre-cultured in culture medium containing 15 mg/L of ZnO-5 and ZnO-5 (15 mg/L) plus Vc (300 mg/L) for 2 h. Cells were collected and washed with PBS and stained by 30 μM TSQ in PBS for 30 min, then washed three times with PBS before analyzed by flow cytometry (FACS, BD Biosciences, USA).

The subcellular location of ZnO NPs and Zn^{2+} in GES-1

Fluorescent labeling of ZnO NPs: Briefly, 4 mg ZnO NPs was dispersed in 3 mL anhydrous dimethylformamide (DMF). A solution of 0.5 Ml amino-propyl-triethoxy-silane (APTS) diluted in 25 μL DMF was added to the particle suspensions, sonicated, and stirred under nitrogen at room temperature for 20 h. The modified NPs were collected by centrifuging and removing the supernatant. After washing, the modified NPs were resuspended in 0.5 mL DMF and mixed with a solution of 1 mg FITC and 0.5 mL DMF. The suspension was stirred for 4 h, and the FITC-labeled NPs were collected by centrifugation. After thoroughly washing of the labeled materials with DMF, the particles were dried under vacuum to remove the organic solvent and stored as dry powders.

Subcellular location of ZnO NPs and Zn^{2+}: Lysosome is a main resident location of metal oxides NPs in cells. Briefly, GES-1 were pre-cultured in culture medium containing 15 mg/L ZnO-5 and ZnO-5 (15 mg/L) plus Vc (300 mg/L) for 2 h or 24 h. The cells were then rinsed two times with PBS and stained for 30 min in an incubator using a solution of 30 μM TSQ in PBS. Then the lysosomes of GES-1 were stained by 1 μM Lyso Tracker (Introgen). After the stained cells were rinsed three times with PBS, the cells were examined under the confocal microscope with an excitation wavelength of 405 nm for TSQ, 488 nm for FITC-ZnO and 635 nm for lysosome.

Measurement of reactive oxygen species: Reactive oxygen species (ROS) were measured using the oxidation-sensitive fluorophore 2′, 7′-dichlorofluorescein diacetate (DCFH-DA, Jiancheng Bioengineering Institute, China). DCFH-DA is a nonfluorescent compound that is freely taken up by cells and hydrolyzed by esterases to 2′, 7′-dichlorofluorescein (DCFH). DCFH is then oxidized to the fluorescent 2′, 7′-dichlorofluorescein (DCF) in the presence of peroxides, thereby indicating the level of intracellular ROS. Briefly, GES-1 were harvested and incubated with 20 mM DCFH-DA dissolved in cell-free medium at 37 °C for 30 min and then washed three times with PBS. Cellular fluorescence was quantified using a fluorescence spectrophotometer (F-700, Hitachi Corp., Japan) at an emission wavelength of 525 nm. Intracellular ROS production was expressed as a percentage of control cell ROS levels.

Measurement of mitochondrial membrane potential: The changes in mitochondrial membrane potential (MMP) were estimated using the fluorescent cationic dye Rhodamine 123 (Sigma-Aldrich, USA). Briefly, GES-1 were washed twice and then incubated with 50 mg/L Rhodamine 123 at 37 ^{o}C for 30 min and washed twice again. The cellular fluorescence intensity of Rhodamine 123 was quantified using fluorescence microplate reader (Thermo, USA) at an excitation wavelength of 485 nm and an emission wavelength of 530 nm. Cellular mitochondrial membrane potential was expressed as a percentage of control cells.

Capase-3 activity assay: Caspase-3 activity was measured through cleavage of a colorless substrate specific for caspase-3 (Ac-DEVD-pNA) releasing the chromophore, p-nitroaniline (pNA). Assays were carried out according to manufacturer's instructions (Beyotime, China). To evaluate the activity of caspase-3, cell lysates were prepared after their respective treatment with various designated treatments. Assays were performed on 96-well microtitre plates by incubating 10 μl protein of cell lysate per sample in 80 μl reaction buffer containing 10 μl caspase-3 substrate (Ac-DEVD-pNA, 2 mM). Lysates were incubated at 37 ^{o}C for 4 h. Samples were measured with microplate reader (Thermo, USA) at an absorbance of 405 nm.

Combined toxicity study in vivo post the oral exposure

Animals and treatments: Sixty male Kunming mice (20 of 60 are 5-6 weeks old 25 ± 2 g and 40 are 3-4 weeks old 15 ± 2 g) were purchased from the Slack Experimental Animal Center (Shanghai, China). All animals were housed by 5 in plastic cages with a stainless steel mesh lid in a ventilated animal room. Room temperature was maintained at 20±2 °C, relative humidity at 60± 10%, and a 12 h light-dark cycle. Distilled water and sterilized food for mice were available ad libitum. Prior to dosing, they were acclimated to this environment for 5 days. All procedures used in this experiment were compliant with the local ethics committee.

We divided these mice into three groups, 20 mice (5-6 weeks old) were in the first group, 20 mice (3-4 weeks old) the second group and 20 mice (3-4 weeks old) the third group. Each group of mice were randomly divided into four experimental groups and treated with different samples: The first and second group were administered orally with 0.2 ml 0.9% NaCl aqueous solution, 14 mg/kg ZnO-5, 50 mg/kg Vc and 14 mg/kg ZnO-5 plus 50 mg/kg Vc twice per day for 30 days. The third group was administered orally with 0.2 ml 0.9% NaCl aqueous solution, 14 mg/kg ZnO-5, 50 mg/kg Vc and 14 mg/kg ZnO-5 plus 50 mg/kg Vc twice per day for 90 days. The dosages of these materials are in accordance with the European food additives standard and Chinese food additives standard. The detailed calculation methods are presented as below. The dosage we used here was calculated according to the state of food and nutrition enhancer standard (GB14880-2012) which declares the dosage of ZnO in infant food is 217 mg/kg. We defined the weight of the infant food was 35 g per bag; the weight of the infant was 10 kg; fed the infant 2 bags once in the morning and evening respectively, then according the equivalent dose ratio of mouse to human beings for 9:1, we admitted the dosage of ZnO was 14 mg/kg. The calculation of Vc was as same as that of ZnO, resulting in a dosage of 50 mg/kg Vc. The limited dosage of Vc was 800 mg/kg. Post exposure, animals in control and experimental groups were weighed and then sacrificed. Blood/organ samples were collected for accumulation determination and toxicological assays. Serum was collected by centrifuging blood at 3,000 rpm for 10 min. The tissues and organs were stored at -80 ^{o}C for other analyses.

Biochemical assays of serum and blood: Liver function was evaluated with levels of total bilirubin levels (TBIL), alanine aminotransferase (ALT) (in ESI), aspartate aminotransferase (AST) (in ESI), alkaline phosphatase (ALP) in serum. Blood urea nitrogen (BUN) and serum creatinine (Cr) (in ESI) were evaluated for nephrotoxicity. All the biochemical parameters were determined according to the methods described in the references by using commercial kits (Nanjing Jiancheng Bioeng Inst., China).

Zinc content analysis: Tissues were taken out of the -80 ^{0}C storage and thawed. About 0.1-0.4 g of each tissue were weighed, digested and analyzed for zinc content analysis. The digestion was first performed in ultrapure nitric acid overnight. After adding 0.5 ml H_2O_2, the mixed solutions were heated at about 180 ^{0}C using high-pressure action container in an oven chamber until the samples were completely digested. Then, the solutions were heated at 120 ^{0}C to remove the remaining nitric acid until the solutions were colorless and clear. At last, the solutions were transferred and diluted to 5 ml with 2% (v/v) nitric acid. The zinc concentration in the digested samples was detected by inductively coupled plasma atomic emission spectrometry (ICP-AES, Leeman Labs., USA).

Gene expression of liver and kidneys: The different gene expression of liver and kidneys post exposure of ZnO NPs, Vc and ZnO NPs plus Vc for 90 days were analyzed by mRNA reverse transcription-polymerase chain reaction (RT-PCR) technique. Herein, we analysed the relative expression level of four kinds of genes: liver fatty acid binding protein (L-FABP), neutrophil gelatinase associated lipocalin (NGAL) and apolipoprotein (APO). Total mRNA of liver was extracted using mRNA extraction kit (Invitrogen). Then the cDNAs were synthesized from the diluted RNA using cDNA synthesis kit (Bioline). The amplification of cDNAs referred to the fluorescent quantitative PCR kit (Bioline) using Real-time detector (ABI-7500, USA). All the operating steps were in strict accordance with the manual.

Statistical Analysis: Results were expressed as the mean ± standard deviation (S.D.) from three to six individual experiments. The statistical significance was analyzed by t-tests of one-way analysis of variance (ANOVA). Difference was considered significant if $p< 0.05$.

Conclusions

We investigated the combined toxicity of ZnO NPs plus Vc for the first time. Vc increased the toxicity induced by ZnO NPs alone both *in vitro* and *in vivo*. Vc also increased the endocytosis processes of ZnO NPs which were resulted from the increase of concentration of Zn^{2+} in cells. The acidity of Vc facilitates the dissolution rate of ZnO NPs in cells. Indubitably, it becomes the predominating mechanism for the increase of Zn ions, hence aggravating cytotoxicity. In the *in vivo* experiments the significant change on the index of liver and kidneys and the change of related protein after repeated oral exposure for three months indicated that the main organs were injured by the mixture of ZnO NPs and Vc. Comparatively, no synergistic toxicity was observed in the case of more chemically inert TiO_2 NPs in a complex system containing Vc. Overall, the nanotoxicology of a composite system requires more attention to fill up the gap of the basic data of the nanofood safety study. Our findings accentuate the importance of the complex system of nanofood, and will stimulate more accurate safety assessments for nanofood in the future.

Acknowledgments

This work is financially supported by the National Basic Research Program of China (973 Program) (No. 2011CB933402), National Natural Science Foundation of China (Nos. 21101104, 21371115 and 11025526), Innovation Program of Shanghai Municipal Education Commission (No. 14YZ025) and Program for Innovative Research Team in University (No. IRT13078).

Notes and references

[a]Institute of Nanochemistry and Nanobiology, Shanghai University, Shanghai 200444, P.R. China,
[b]Beijing National Laboratory for Molecular Sciences, Department of Chemical Biology, College of Chemistry and Molecular Engineering, Peking University, Beijing 100871, P. R. China. *e-mail: yliu@pku.edu.cn; mhwu@shu.edu.cn.

1 T. V. Duncan,*Nat. Nanotechnol.*, 2010, **6**, 683-688.
2 X. X. Chen, B. Cheng, Y. X. Yang , A. Cao, J. H. Liu, J. H. Du, Y. Liu, Y. Zhao and H. Wang, *Small*,2013, **9**, 1765-1774.
3 K. Lau, W. G. McLean, D. P. Williams and C. V. Howard, *Toxicol. Sci.*, 2006, **90**, 178-187.
4 H. Shi, R. Magaye, V. Castranova and J. Zhao, *Part. FibreToxicol.*, 2013, **10**, 15.
5 Y. Wang, Q. X. Wu, K. Sui, X. X. Chen, J. Fang, X. Hu, M. Wu and Y. Liu, *Nanoscale*, 2013, **5**, 4737-4743.
6 A. K. Suresh, D. A. Pelletier, W. Wang, J. L. Morrell-Falvey, B. H. Gu and M. J. Doktycz, *Langmuir*, 2012, **28**, 2727-2735.
7 Y. Pan, S. Neuss, A. Leifert, M. Fischler, F. Wen, U. Simon, G. Schmid, W. Brandau and W. Jahnen-Dechent, *Small*, 2007, **11**, 1941-1949.
8 S. K. Sohaebuddin, P. T. Thevenot, D. Baker, J. W. Eaton and L. P. Tang, *Part. FibreToxicol.*, 2010, **7**,22.
9 A. Martirosyan, A. Bazes and Y. J. Schneider, *Nanotoxicology*, 2014, **8**, 573-582.
10 B. Guo, R. Zebda, S. J. Drake and C. M. Sayes, *Part. FibreToxicol.*, 2009,**6**, 4.
11 A. Llorens, E. Lloret, P. A. Picouet, R. Trbojevich and A. Fernandez, Trends. *Food Sci. Tech.*, 2012, **24**, 19-29.
12 S. F. Hansen, E.S. Michelson, A. Kamper, P. Borling, F. Stuer-Lauridsen and A. Baun, *Ecotoxicology*, 2008, **17**, 438-447.
13 A. S. Prasad, *Exp.Gerontol.*, 2008, **43**, 370-377.
14 C. Andreini, L. Banci, I. Bertini and A. Rosato, *J. Proteome Res.*, 2006, **5**, 3173-3178.
15 C. Andreini, L. Banci, I. Bertini and A. Rosato, *J. Proteome Res.*, 2006, **5**, 196-201.
16 M. J. Rincker, G. M. Hill, J. E. Link, A. M. Meyer and J. E. Rowntree, *J. Anim. Sci.*,2005, **83**, 2762-2774.
17 B. Wu, Y. Wang, Y. Lee, A. Horst, Z. Wang, D. Chen, R. Sureshkumar and Y. J. Tang, *Environ. Sci. Technol.*, 2010, **44**, 1484-1489.
18 P. J. P. Espitia, N. F. F. Soares, J. S. R. Coimbra, N. J. Andrade, R. S. Cruz and E. A. A. Medeiros,*Food Bioprocess Tech.*, 2012, **5**,1447-1464.
19 M. Mortimer, K. Kasemets and A. Kahru, *Toxicology*, 2010, **269**, 182-189.
20 M. Xu, F. Daisuke, K. Shoko, M. Takashi, X. Li, T. Taro, I. Hideo and H. Nobutaka, *Biomaterials*, 2010, **31**, 8022-8031.
21 S. T. Yang, J. H. Liu, J. Wang, Y. Yuan, A. Cao, H. Wang, Y. Liu and Y. Zhao, *J. Nanosci. Nanotechno.*, 2010, **10**, 8638-8645.
22 W. Lin, Y. Xu, C. C. Huang, Y. Ma, K. B. Shannon, D. R. Chen and Y. W. Huang, *J. Nanopart. Res.*, 2009, **11**, 25-39.
23 H. Wang, R. L. Wick and B. Xing, *Environ. Pollut.*, 2009, **157**, 1171-1177.
24 B. Frei, L. England and B. N. Ames, *Proc. Natl. Acad. Sci. U. S. A.*, 1989, **86**, 6377-6381.
25 B. Frei, R. Stocker, L. England and B. N. *Ames, Adv. Exp. Med. Biol.*, 1990, **264**,155-163.
26 F. Wei, C. Qu, T. Song, G. Ding, Z. Fan, D. Liu, Y. Liu, C. Zhang, S. Shi and S. Wang, *J. Cell Physiol.*, 2011, **227**, 3216-3224.
27 B. Halliwell, *Free Rad. Res.*, 1996, **25**, 439-454.
28 A. Kumar, A. Rahal, R. Mandil and A. Prakash, *Toxico. Enviro. Chem.*, 2013, **95**, 1595-1610.
29 L. F. Verde, G. S. Lopes, S. S. M. Ihara, N. H. Jurkiewicz and A. Jurkiewicz, *Eur. J. Pharmacol.*, 2014, **735**, 211-218.
30 L. Shao, L. T. Young and J. F. Wang, *Biol. Psychiatry.*, 2005, **58**, 879-884.
31 Y. Wang, L. Yuan, C. Yao, L. Ding, C. Li, J. Fang and M. Wu, *RSC Adv.*, 2014, **4**,42168-42174
32 M. Christophe and S. Nicolas, *Curr. Pharm. Des.*, 2006, **12**, 739-757.
33 W. G. Tatton and C. W. Olanow, *Biochim. Biophys. Acta. Bioenerg.*, 1999, **1410**, 195-213.
34 J. E. Ricci, R. A. Gottlieb and D. R. Green, *J. Cell Biol.*, 2003, **160**, 65-75.
35 K. Kasemets, A. Ivask, H. C. Dubourguier, A. Kahru, *Toxicol. In Vitro*, 2009, **23**, 1116-1122.
36 M. Heinlaana, A. Ivask, I. Blinova, H. C. Dubourguier and A. Kahru, *Chemosphere*, 2008, **71**, 1308-1316.
37 T. Xia, M. Kovochich, M. Liong, L. Mädler, B. Gilbert, H. Shi, J. I. Yeh, J. I. Zink and A. E. Nel, *ACS Nano*, 2008, **2**, 2121-2134.
38 J. W. Meeusen, H. Tomasiewicz, A. Nowakowski and D. H. Petering, *J. Inorg. Biochem.*, 2011, **50**, 7563-7573.
39 ATSDR Toxicological Profile for Zinc. US Department of Health and Human Services, Public Health Service, Agencyfor Toxic Substances and Disease Registry, 2005.
40 J. W. Moreau, P. K. Weber, M. C. Martin, B. Gilbert, I. D. Hutcheon and J. F. Banfield, *Science*, 2007, **316**,1600-1603.

41 F. Zhao, Y. Zhao, Y. Liu, X. Chang, C. Chen and Y. Zhao, *Small*, 2011, **7**,1322-1337.
42 B. D. Chithrani and W. C. W. Chan, *Nano Lett.*, 2007, **7**, 1542-1550.
43 K. K. Liu, C. C. Wang, C. L. Cheng and J. I. Chao, *Biomaterials*, 2009, **30**, 4249-4259.
44 H. F. Oshrat, R. Eva, B. Simon and A. Yoram, *Biomacromolecules*, 2008, **9**, 435-443.
45 N. W. S. Kam, T. C. Jessop, P. A. Wender and H. J. Dai, *J. Am. Chem. Soc.*, 2014, **126**, 6850-6851.
46 D. Pantarotto, R. Singh, D. McCarthy, M. Erhardt, J. P. Briand, M. Prato, K. Kostarelos, *A. Bianco, Angew. Chem. Int. Ed.*, 2004, **43**, 5242-5246.
47 S. E. A. Gratton, P. A. Ropp, P. D. Pohlhaus, J.C. Luft, V. J. Madden, M. E. Napier and J. M. DeSimone, *Proc. Natl. Acad. Sci. U. S. A.*, 2008, **105**, 11613-11618.
48 R. Tedja, M. Lim, R. Amal and C. Marquis, *ACS Nano*, 2012, **6**,4083-4093.
49 J. M. McKim, *Crit. Rev. Toxicol.*, 2014, **44**, 211-243.
50 T. Shimamura, S. Iijima, M. Hirayamac, M. Iwashita, S. Akiyama, Y. Takaku and S. Yumoto, *Biochemistry*, 2013, **27**, 12-20.
51 U. Aksu, R. Bezemer, B. Yavuz, A. Kandil, C. Demircib and C. Ince, *Resuscitation* , 2012, **83**,767-773.
52 J. Cai, C. Lücke, Z. Chen, Y. Qiao, E. Klimtchuk and J. A. Hamilton, *Biophys. J.*, 2012, **102**, 2585-2594.
53 H. Oda, Y. Suzuki, M. Wakayama and A. Yoshida, *J. Nutr. Biochem.*, 2000, **11**, 568-573.
54 A. Weir, P. Westerhoff, L. Fabricius, K. Hristovski and N. Goetz, *Environ. Sci. Technol.*, 2012, **46**, 2242-2250.
55 G. Oberdoester, *Philos. Trans. R. Soc. London A*, 2000, **358**, 2719-2740.
56 T. N. Siegel, D. R. Hekstra and G. A. M. Cross, *Mol. Biochem. Parasit.*, 2008, **160**, 171-174.

The table of contents entry

We investigated the combined toxicity of zinc oxide nanoparticles and Vitamin C (ascorbic acid). The results showed that Vc increased the cytotoxicity significantly compared with that of the single ZnO NPs.

TOC Keyword: combined toxicity

Combined toxicity study of zinc oxide nanoparticles and Vitamin C in food additives

Y. Wang[a], L. Yuan[a], C. Yao[a], L. Ding[a], C. Li[a], J. Fang[a], K. Sui[a], Y. Liu[b]*, M. Wu[a]*

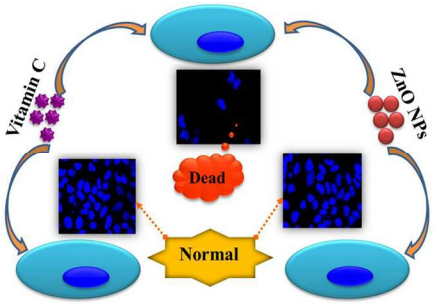

Page Headings
Left page: Y. Wang *et al.*
Right page: Combined toxicity study of ZnO NPs and Vc